

# Cross-sectional classification of aluminium beams subjected to fire

O. R. van der Meulen \* † ‡, J. Maljaars ‡ and F. Soetens †‡

\* Materials innovation institute (M2i), Delft, the Netherlands

† Faculty of Architecture, Building and Planning, Eindhoven University of Technology, Eindhoven, the Netherlands

‡ TNO Built Environment and Geosciences, Delft, the Netherlands

The use of aluminium as a construction material has been increasing since its first invention. At present, limited knowledge of the behaviour of aluminium beams in fire gives rise to excessively high insulation demands, decreasing its competitiveness. An explorative study is presented here that aims to assess the potential for improvement in the existing design standards for aluminium in fire conditions. At present, fire design for aluminium alloy beams is performed using the same system of cross-sectional slenderness classes as is employed at room temperature. Identical width-over-thickness ratio limits are used to define the boundaries between the classes. These limits are known (and demonstrated) to be conservative, but may in fact be over-conservative. Especially for tempered alloys, the geometric limits may be relaxed considerably, allowing cross-sections to be upgraded in class for fire design calculations.

*Key words: Aluminium, fire, cross-sectional classification, rotation capacity, curvature localization*

## 1 Introduction

The design of aluminium bending members in fire according to the European standard for structural fire design in aluminium structures (EN 1999-1-2, 2007) follows the same cross-sectional classification system as the standard for room temperature design (EN 1999-1-1, 2007). The two standards also share a single set of geometric limits to the boundaries between the four classes. This is a conservative assumption, but it is over-conservative in many instances as the resistance to local buckling increases and the required curvature to achieve redistribution of forces decreases with an increase in temperature. In this paper a study is performed to increase the geometric limits of the different cross-sectional boundaries. Failure is considered to occur through local buckling

of the constituent plates only; tensile failure and lateral torsion buckling are assumed to be prevented by the choice of material and support conditions.

To introduce the reader to a number of concepts pertaining to this study, an introduction is given into aluminium and its alloys, and the concepts of cross-sectional classification and rotation capacity. Class 2, 3 and 4 cross-sections in fire conditions are then discussed in section 2. For class 1, a phenomena called 'curvature localization' plays a significant role. This phenomena and its effect on the geometrical limits of class 1 cross-sections is dealt with in section 3. To demonstrate the significance of the concepts discussed in this article, a worked out example is given in section 4. Lastly, conclusions are offered in section 5.

### *1.1 Aluminium alloys*

Aluminium is often alloyed with other elements to improve properties such as its strength. A four digit number issued by the Aluminum Association is used to designate the different alloys, where the first number indicates the mayor alloying element. In the (marine) construction industry, mainly AA5xxx and AA6xxx alloys are used. In these industries, one of the most popular alloys for sheet products is AA5083, and for extrusions AA6060 or AA6082.

#### *Work and precipitation hardening*

Aluminium alloys are often treated mechanically or by means of heat to increase their strength. These two processes are explained hereafter.

- Work hardening or 'cold working' of a material is a process where the material is deformed plastically to generate additional defects or dislocations in the metal structure, these dislocations pile up and impede further plastic deformation which results in a higher yield strength of the material. When an aluminium product has received such a treatment or *temper*, this is indicated by an 'Hxxx' behind the four digit designation of the alloy used, where 'xxx' is a number indicating the amount of work hardening applied.
- Precipitation hardening is a temper that is only possible for alloys specifically engineered for this purpose. One or more of the alloying agents is added in a quantity that is completely soluble in aluminium when the aluminium is liquid, but has to precipitate out partially when the alloy is cooled to room temperature. This precipitation process forms clusters of alloying atoms that hamper deformation

much like the defects of the work hardening process. The precipitation process takes time to complete however, and this is why *naturally aged*, precipitation hardened alloys (as designated with a 'T4' behind the alloy number for example) increase in yield stress over time. The process can also be finished during production in a matter of hours by heating the material to a temperature in the range of 120°C-180°C. A temper designation 'T6' or 'T66', amongst others, indicates that an alloy has received such an artificial aging heat treatment.

If the alloy did not receive a temper, or if it has been subjected to a temperature above the recrystallization temperature after tempering, the alloy is said to be in an annealed condition, or as having a '0-temper'.

### 1.2 Cross-sectional classification

The European standard for aluminium design (EN 1999-1-1, 2007), like many other modern design standards, employs a system of cross-sectional classification for members in bending. Based on the geometry of the cross-section, expressed as the width-over-thickness ratio ( $b/t$  or  $\beta$ ) of the constitutive plates, members are classified to be of class 1, 2, 3 or 4. The maximum allowable stress and the possibility for plastic design depends on the class of the cross-section.

- Class 4, the most slender class of cross-section. The conventional elastic moment  $M_{0,2}$  is not reached. The maximum moment  $M_{rd}$  is reduced following an effective area approach.
- Class 3, semi compact sections.  $M_{0,2}$  is reached, but not the plastic moment  $a_0M_{0,2}$ . The moment  $M_{rd}$  is equal to the elastic moment  $M_{0,2}$ .
- Class 2, compact sections. The plastic moment  $a_0M_{0,2}$  is reached, but the moment decreases too fast at greater curvatures to allow plastic design.  $M_{rd}$  is equal to  $a_0M_{0,2}$ .
- Class 1, ductile sections. The plastic moment  $a_0M_{0,2}$  is reached and the moment stays above the conventional elastic moment  $M_{0,2}$  for at least a certain specified rotation capacity. This allows for plastic design rules and the redistribution of forces. The normative part of (EN 1999-1-1, 2007) sets  $M_{rd}$  equal to  $a_0M_{0,2}$ .

$a_0$  is the geometric shape factor equal to the quotient of the plastic- and the elastic-section modulus. A graphical representation of the four cross-sections is given in figure 1a.

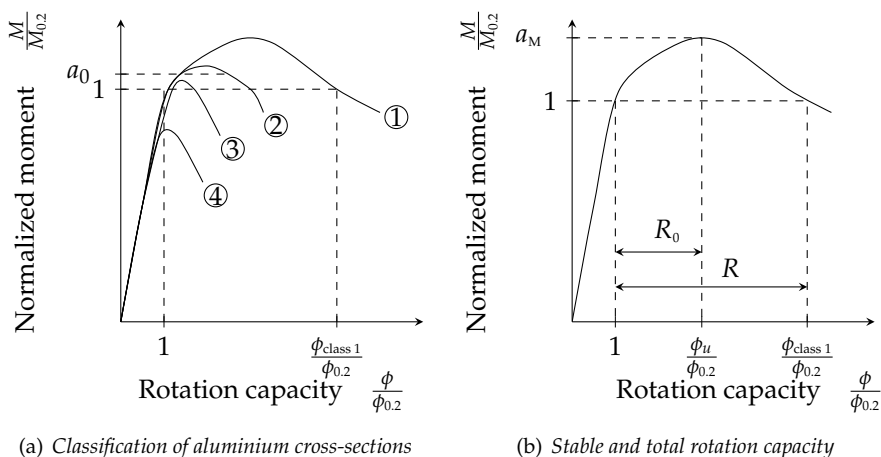


Figure 1: (a) Classification of aluminium cross-sections after (EN 1999-1-1, 2007). The numbers in the circles indicate the cross-sectional class. (b) Difference between stable and total rotation capacity, after: (Mazzolani and Piluso, 1995).

### 1.3 Rotation capacity

As mentioned in the previous section, the boundary between sections of class 1 and 2 is defined on the basis of their rotation capacity. With regard to rotation capacity some ambiguity exists in nomenclature and the relevant terms are defined here therefore. The stable rotation capacity  $R_0$  is the rotation where the calculated ultimate moment  $M_u$  is reached, decreased by, and normalized to, the elastic rotation capacity, as given in equation (1) and as demonstrated in figure 1b.

$$R_0 \equiv \frac{\phi_u}{\phi_{0.2}} - 1. \quad (1)$$

The ‘regular’ rotation capacity  $R$  is based on the rotation where the moment, after local-buckling has occurred, dips below the elastic moment again. This definition deviates from steel design where the plastic moment is commonly set as the second boundary.

The answer to the question whether the stable rotation capacity  $R_0$ , or the total rotation capacity  $R$  should be used to define the boundary between classes 1 and 2, depends on the plastic design rules used afterwards. The actual minimum required capacity according to either limit is always somewhat arbitrary, as it depends on how inefficient a structure with regard to plastic design we are willing to consider. The use of the total rotation capacity  $R$  as a limit is most appropriate when we do not take into account strain hardening and

assume a constant plastic moment. The stable rotation capacity  $R_0$  should be used if an increase in moment past the plastic moment is considered in the subsequent strength calculations. The Eurocode (EN 1999-1-1, 2007; EN 1999-1-2, 2007) is implicitly based on a stable rotation capacity  $R_0$  equal to 3 (De Matteis et al., 2003; Mazzolani et al., 1996), but does not consider the increase in moment past the plastic moment in the formal part of the standard. In its informative Annex F however, a procedure is given which does take this increase into account. The moment used in the plastic strength calculation according to either method may be calculated through

$$M_u = a_{M,1} W_{el} f_d, \quad (2)$$

where  $a_{M,1}$  is equal to the generalized shape factor  $a_0$  according to the formal part of the standard. The informative annex (EN 1999-1-1, 2007, Annex F) sets it equal to  $a_5$  or  $a_{10}$ , depending on the tensile ductility class of the alloy, as defined in the before mentioned informative annex.

$$a_5 = 5 - \frac{3.89 + 0.00190 n}{a_0^{0.270 + 0.0014 n}}, \quad (3)$$

$$a_{10} = a_0^{0.21 \log(1000 n)} 10^{0.0796 - 0.0809 \log\left(\frac{n}{10}\right)}. \quad (4)$$

Equations (3) and (4) were derived by Cappelli et al. (1987) from a curve fit of ‘... numerical simulation to a wide range of cases’.

The moment curvature relationship is a convenient tool to study the behaviour of bending members. For aluminium alloy bending members an approximation formula is given in (EN 1999-1-1, 2007, Annex G) and (Cappelli et al., 1987):

$$\frac{\kappa}{\kappa_{0.2}} = \frac{M}{M_{0.2}} + k \left( \frac{M}{M_{0.2}} \right)^m, \quad (5)$$

where  $\kappa_{0.2}$  and  $M_{0.2}$  denote the curvature and moment, respectively, where the 0.2% proof stress is first reached in any part of the cross-section.

$$m = \frac{\log\left(\frac{10 - a_{10}}{5 - a_5}\right)}{\log\left(\frac{a_{10}}{a_5}\right)}, \quad (6)$$

$$k = \frac{5 - a_5}{a_5^m} = \frac{10 - a_{10}}{a_{10}^m}. \quad (7)$$

## 2 Classes 2, 3 and 4 in fire conditions

As already stated in the introduction, the geometrical limits to the boundaries of the four cross-sectional classes at room temperature (EN 1999-1-1, 2007), are used for the elevated temperatures associated with fire as well (EN 1999-1-2, 2007). This was shown to be a conservative approach by Lundberg (2003) for all but one alloy tested, for which a negligible degree of un-conservativeness was found. The influence of the temperature on the geometrical limits to the cross-sectional classes can be calculated by taking the expression for the width-over-thickness ratio ( $b/t$  or  $\beta$ ) of the plates constituting the cross-section at room temperature:

$$\beta \equiv \frac{b}{t} = C\hat{\varepsilon}, \quad (8)$$

where  $C$  is an empirical constant for the given cross-sectional class limit and  $\hat{\varepsilon}$  is a constant expressing the influence of the material defined as

$$\hat{\varepsilon} \equiv \sqrt{\frac{250}{f_{0.2}}}, \quad \text{where } f_{0.2} \text{ is in } MPa, \quad (9)$$

where, to avoid ambiguity, the Eurocode notation  $\varepsilon = \hat{\varepsilon}$  is avoided. The constant 250 is a linear function of the Young's modulus  $E$  and 'the different constants used for calculating the slenderness parameters' (Lundberg, 2003). The value of  $\beta$  at elevated temperatures is denoted by  $\beta_\theta$  and may be expressed by

$$\beta_\theta = \beta \frac{\hat{\varepsilon}_\theta}{\hat{\varepsilon}}, \quad (10)$$

where  $\hat{\varepsilon}_\theta$  is the value of  $\hat{\varepsilon}$  at elevated temperatures. The ratio between the two constants is given in (Lundberg, 2003) as

$$\frac{\hat{\varepsilon}_\theta}{\hat{\varepsilon}} = \frac{\sqrt{\frac{250k_{E,\theta}E}{70000k_{0.2,\theta}f_{0.2}}}}{\sqrt{\frac{250E}{70000f_{0.2}}}} = \sqrt{\frac{k_{E,\theta}}{k_{0.2,\theta}}}, \quad (11)$$

where  $k_{E,\theta}$  and  $k_{0.2,\theta}$  are reduction factors given in (EN 1999-1-2, 2007), expressing the value of the Young's modulus and 0.2% proof stress at elevated temperatures, respectively, normalized to their value at room temperature. Combining equation (10) and (11) yields:

$$\frac{\beta_\theta}{\beta} = \frac{\hat{\varepsilon}_\theta}{\hat{\varepsilon}} = \sqrt{\frac{k_{E,\theta}}{k_{0.2,\theta}}}. \quad (12)$$

Unlike steel, the ratio  $\hat{\varepsilon}_\theta/\hat{\varepsilon}$  is almost invariably greater than unity for aluminium alloys, which is caused by  $k_{E,\theta}$  being equal to, or larger than  $k_{0.2,\theta}$ , for all but one of the researched

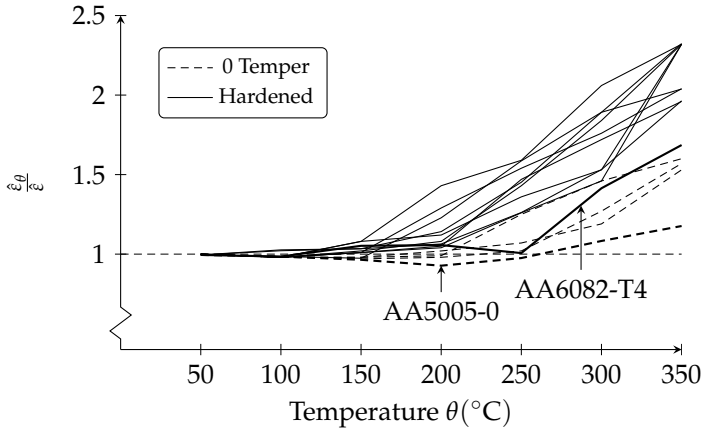


Figure 2: The ratio  $\hat{\varepsilon}_\theta / \hat{\varepsilon}$  as a function of the temperature for the aluminium alloys as given in (EN 1999-1-2, 2007, Table 1a). Among the alloys drawn are the AA 5083-0/H12/H22/H32, AA 6060 T6/T66 and AA 6082-T4/T6 alloys. The lowest value is found for AA 5005-0; 0.927 at 200°C. The lowest value, when not taking into account this alloy, is 0.97.

aluminium alloys. This means that a cross-sectional classification system based on the room temperature derived limits to  $\beta$  is conservative for fire design, but may be over-conservative, as is shown in figure 2, for all alloys in (EN 1999-1-2, 2007, Table 1a).

Figure 2 demonstrates the increase in stability of aluminium alloys at elevated temperatures. A notable exception is aluminium alloy AA5005-0, which has a 7% reduction in  $\beta$  at around 200°C. While the increase in maximum  $\beta$  can be relatively modest for 0-temper alloys (between 8% and 46% at 300°C), a distinct increase is present for work and precipitation hardened alloys (between 46% and 106%). An exception to this is AA6082-T4, which has a lower increase in  $\beta$  due to its high values for  $f_{0.2}$  at temperatures in the range of 200°C to 300°C. This is caused by the naturally aged T4 temper effectively receiving an artificial heat treatment by the fire. Given the increase in maximum  $\beta$  for work and artificially aged precipitation hardened alloys, it is feasible to derive a scheme to increase the geometric limits for these particular alloys at elevated temperatures. A simple and conservative approximation for these alloys as present in figure 2 is given by

$$\frac{\beta_\theta}{\beta} = \frac{\hat{\varepsilon}_\theta}{\hat{\varepsilon}} = \begin{cases} 0.16 + 0.0042 \theta, & \text{for } 200 \leq \theta \leq 350^\circ\text{C} \\ 1, & \text{for } \theta < 200^\circ\text{C} \end{cases} \quad (13)$$

### 3 Class 1 in fire conditions

The geometrical limit to class 1 cross-sections at room temperature was derived from stub column compression tests such as described in (Mazzolani et al., 1996) and (Faella et al., 2000) for square and rectangular hollow members. The ratio of the local buckling strain over the elastic strain was found to behave according to (Faella et al., 2000)

$$\frac{\varepsilon_{cr}}{\varepsilon_{0.2}} = \frac{0.905 k}{\hat{\beta}^{C_1+C_2 \hat{\beta}}}, \quad (14)$$

where  $\hat{\beta}$  is defined as

$$\hat{\beta} = \frac{b}{t} \sqrt{\frac{f_{0.2}}{E}}, \quad (15)$$

and  $k$  is equal to 4. The constants  $C_1$  and  $C_2$  are equal to 2.28 and 0.16, respectively. This is close to the analytical solution, for which  $C_1$  is equal to 2 and  $C_2$  to 0. The theoretical buckling strain equation is given below, which is subsequently rewritten to  $\beta$ .

$$\varepsilon_{cr} = \frac{k\pi^2}{12(1-\nu^2)} \left(\frac{1}{\hat{\beta}}\right)^2 \Rightarrow \beta = \sqrt{\frac{\varepsilon_{0.2}}{\varepsilon_{cr}}} \sqrt{\frac{1}{\varepsilon_{0.2}}} \sqrt{\frac{k\pi^2}{12(1-\nu^2)}}. \quad (16)$$

Using equation (12), this is rewritten to a temperature dependent form, and then the quotient of the value for  $\beta$  at elevated temperatures to its room temperature value is obtained.

$$\beta = \sqrt{\frac{k_E(\theta)}{k_{0.2}(\theta)}} \frac{1}{\sqrt{\frac{\varepsilon_{cr}(\theta)}{\varepsilon_{0.2}(\theta)}}} \sqrt{\frac{E}{f_{0.2}}} \sqrt{\frac{k\pi^2}{12(1-\nu^2(\theta))}} \Rightarrow \frac{\beta_\theta}{\beta} = \underbrace{\frac{\sqrt{1-\nu^2}}{\sqrt{1-\nu_\theta^2}}}_{\nu \text{ part}} \underbrace{\sqrt{\frac{k_{E,\theta}}{k_{0.2,\theta}}}}_{k \text{ part}} \underbrace{\sqrt{\frac{\frac{\varepsilon_{cr}}{\varepsilon_{0.2}}}{\left(\frac{\varepsilon_{cr}}{\varepsilon_{0.2}}\right)_\theta}}}_{\text{req. capacity}}. \quad (17)$$

It is noted that equation (17) represents the theoretical case for which  $C_1$  is equal to 2 and  $C_2$  is 0 in equation (14). It is not possible to derive an analytical solution with the empirically derived constants  $C_1$  and  $C_2$  equal to 2.28 and 0.16. It is however possible to solve the equations numerically and the behaviour is very close to the analytical case.

The Poisson's ratio was assumed to be equal to 0.5 for buckling in the plastic range. Especially for slender sections, this value may be too high. It is known the Poisson's ratio increases for aluminium alloys at elevated temperatures (Maljaars, 2008; Maljaars et al., 2010), but exact data is scarce and is characterized by a significant spread. We may set the 'v-part' of equation (17) equal to unity, incurring a maximum degree of over-conservativeness of 10% based on a Poisson's ratio equal to 0.3 at room temperature and 0.5 in fire conditions. This simplification is never unconservative.

The  $k$ -part of equation (17) expresses the influence of the decrease in stiffness and strength at elevated temperatures relative to each other. In this part we recognize equation (12), and therefore figure 2 and equation (13) hold within the same set of conditions. The influence of the  $k$ -part is thus generally positive and can be described by equation (13) for work and precipitation hardened alloys with the exception of naturally aged varieties.

The required rotation capacity part of equation (17) describes the influence of a changing deformation demand at elevated temperatures. Class 1 alloys are different to the other classes in the sense that plastic design rules may be employed without further verification of ductility. As was described before, this was done by specifying a value for the stable rotation capacity  $R_0$ . This value corresponds to a structure with a certain degree of inefficiency with regard to plastic design. As will be shown hereafter, the required amount of ductility necessary for a plastic mechanism to be able to form is highly dependent on the strain-hardening potential of the alloy through a phenomenon known as curvature localization. This will be discussed below, after describing the increase in strain hardening potential of aluminium alloys at elevated temperatures first.

### 3.1 Strain hardening at elevated temperatures

The stress-strain law of round-house materials like aluminium alloys are commonly described by the well known Ramberg-Osgood (Ramberg and Osgood, 1943) equation.

$$\varepsilon = \frac{\sigma}{E} + \varepsilon_e \left( \frac{\sigma}{f_{0.2}} \right)^n, \quad (18)$$

where the exponent  $n$  expresses the amount of strain hardening. Work- and precipitation-hardened alloys receive their increase in 0.2% proof stress  $f_{0.2}$  at the expense of their strain-hardening potential, leading to high values for  $n$ . In fire conditions, however, the strain-hardening potential is regained as the different tempers all tend to the annealed condition. This leads to a lower value for  $n$ , as was demonstrated by Maljaars et al. (2010) for both a work- and a precipitation-hardened alloy, AA5083-H111 and AA6060-T66, respectively. The value for  $n$  is given by

$$n = \begin{cases} 8.8 - 0.016\theta, & \text{for AA5083-H111 and } 175 \leq \theta \leq 350^\circ\text{C} \\ 19 - 0.04\theta, & \text{for AA6060-T66 and } 175 \leq \theta \leq 350^\circ\text{C} \end{cases} \quad (19)$$

The room temperature values are given by (EN 1999-1-1, 2007) as equal to 5 and 16-18, respectively.

### 3.2 Curvature localization

Bending members subjected to a non-constant moment, such as the simply supported beam with a single central load as depicted in figure 3a, suffer from a phenomenon known as ‘curvature localization’ (Moen, 1999); which is the tendency of the bulk of the curvature to be concentrated into small regions of the beam. The effect is strongest for materials without strain hardening ( $n = \infty$ , or elastic perfect-plastic, as steel is often modelled to behave as, within the scope of stability calculations) and these theoretically localize all plastic curvature into hinges of an infinitely small linear dimension. For materials with an increasing amount of strain hardening, the effect of curvature localization decreases, and both the localization zone and the curvatures are finite. This difference in behaviour, and the consequences this has for the required rotation capacity of a beam under a varying moment, is discussed below.

All plates comprising a total cross-section have a strain  $\epsilon_{lb}$ , for which local buckling occurs, from this a certain maximum curvature can be derived, at which the first plate starts to buckle. The local buckling strain, and hence curvature, are higher for a material with more strain hardening potential. To illustrate the effect of curvature localisation, we will assume an equal local buckling curvature  $\kappa_{lb}$  however. In reality, the effect of curvature localization will be amplified by the mentioned increase in maximum curvature. Figure 3c shows the moment distribution for a weak strain-hardening material with  $n = 30$  and a strong strain-hardening material with  $n = 5$ . The ultimate moments  $M_{u,n=5}$  and  $M_{u,n=30}$  relative to an equal value for  $M_{0,2}$ , were obtained from equation (5) as a function of the assumed curvature  $\kappa_{lb}$  relative to the elastic curvature  $\kappa_{0,2}$  value of 5 and an assumed geometrical shape factor  $a_0$ , equal to 1.5.

From this figure it is clear that, as the strain hardening is increased, the maximum allowable moment goes up as well. A more dramatic effect can be seen in the curvature distribution as shown in figure 3b, which is also derived from equation (5). Due to the effect of curvature localization, the weak strain hardening material is restricted to elastic values for most of its length, with a narrow zone of plastic behaviour only, while the strong strain hardening material is able to plastically deform along a far greater length. Integrating these curvature profiles yields the deformation of both members, along with the rotation at the supports, as shown in figure 3d. From this figure it is apparent that the maximum rotation at the supports, and thus the (stable) rotation capacity is much larger for beams with an increased amount of strain hardening in case of a variable moment across the beam.

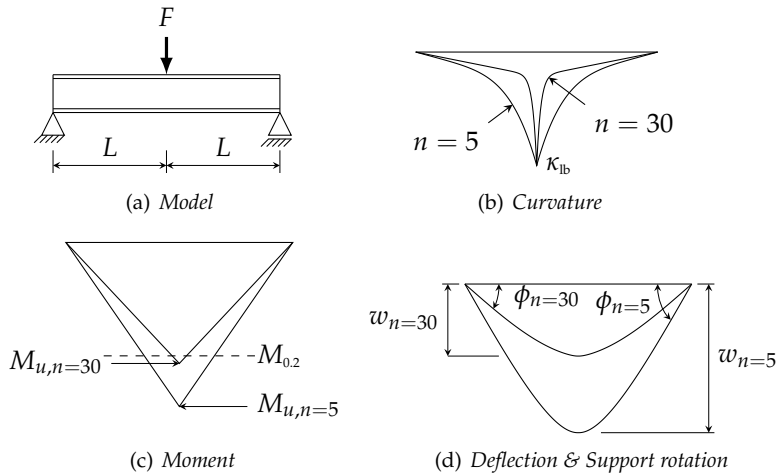


Figure 3: The principle of localization and its effect on the rotation capacity of a beam under a moment gradient, for a heat treated aluminium alloy with  $n = 30$  with little strain hardening, and an aluminium alloy without heat treatment ( $n = 5$ ) and a considerable amount of strain hardening.

It was already shown in the previous section that the strain-hardening potential is increased at elevated temperatures. In this section it was found that the effect of curvature localization is less for materials with a greater amount of strain-hardening. For structures at elevated temperatures, the required ductility is thus less, and the influence of the required capacity part of equation (17) is a positive one. To quantify this effect, we will take a look at a more complex structure; the three span continuous beam, which is argued to be able to describe a wide range of structural types. Before this, the concept of curvature capacity is introduced.

### 3.3 Curvature capacity

For an elastic perfect-plastic material, the (stable) rotation capacity is directly proportional to the rotation in the first appearing plastic hinge because all the plastic curvature is restricted to infinitely small hinges. This makes rotation capacity a convenient way of describing the required ductility of a beam; it has a constant, material and cross-section independent, value for a given beam and load geometry, and it has a direct relationship to the rotation in the first appearing plastic hinge. For round-house materials, this is no longer the case. It is exceeding a certain maximum curvature with associated cross-sectional plate strains which leads to local buckling. The plastic deformation capacity is thus expressible by a curvature capacity, which is a cross-sectional property only.

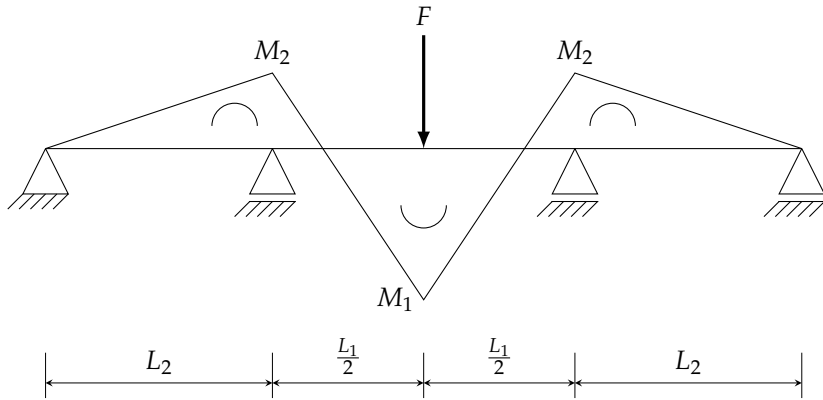


Figure 4: The elastic moment distribution in a three-span continuous beam due to a single concentrated force at the centre of the middle span.

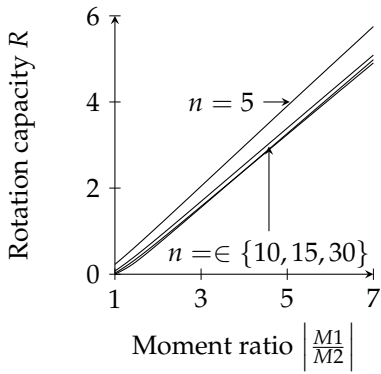
The *required* curvature for a certain beam and load geometry is, for round-house materials, not an exclusive beam/load combination property, but is also dependent on the strain-hardening potential of the alloy through the effect of curvature localization; beams with less localized hinges require a lower maximum curvature. A way of comparing between bending members of equal ductility demand is the curvature capacity  $R_\kappa$  which is defined as

$$R_\kappa \equiv \frac{\kappa_{lb}}{\kappa_{0.2}} - 1. \quad (20)$$

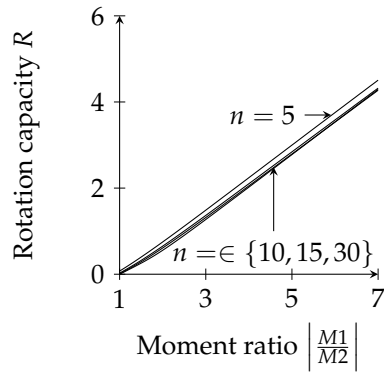
### 3.4 Curvature distribution in a 3-span continuous beam

To study the required rotation capacity of real life structures, a model structure is required which needs multiple plastic hinges to develop before collapse occurs. A versatile type of structure, capable of simulating a wide range of structures is the 3-span continuous beam of figure 4. In this figure, the elastic moment distribution due to a single concentrated force at the centre of the middle beam is shown. The ratio between the elastic moments  $|M_1/M_2|$  is identical to the ratio between the rotations in the first occurring plastic hinge to the second, in case all rotations are assumed to be restricted to plastic hinges. The ratio  $|M_1/M_2|$  is therefore expected to have an approximately linear relation to the required rotation capacity. The ratio  $|M_1/M_2|$  itself is a function of the geometry, and can be modified by changing the ratio between the lengths of the centre and the side spans through

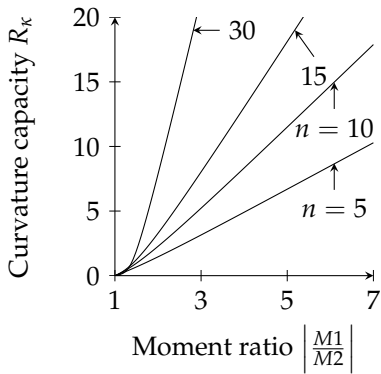
$$\left| \frac{M_1}{M_2} \right| = \frac{1}{\frac{3}{4} \frac{L_1}{L_2}} + 1. \quad (21)$$



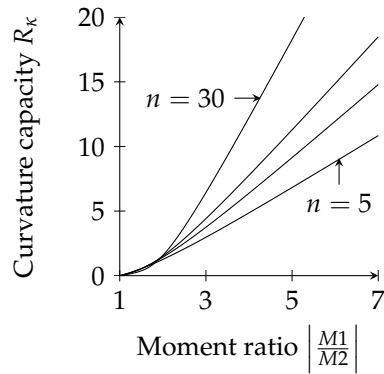
(a) Influence on  $R$ ,  $a_0 = 1.15$



(b) Influence on  $R$ ,  $a_0 = 1.5$



(c) Influence on  $R_\kappa$ ,  $a_0 = 1.15$



(d) Influence on  $R_\kappa$ ,  $a_0 = 1.5$

Figure 5: Influence of moment ratio  $|M1/M2|$  as defined in figure 4, on the rotation and curvature capacity requirements for a symmetric three-span continuous beam.

Similar equations were derived for other structural types, and through the  $|M1/M2|$  ratio we can represent them all. A numerical procedure is employed to derive the moment and curvature distribution of the before mentioned 3-span continuous beam, based on equation (5). When we vary the ratio  $|M1/M2|$ , the required rotation capacity  $R$  reacts approximately linear as predicted. This is shown in figures 5a and 5b. There appears to be little influence of the exponent  $n$  or the geometrical shape factor  $a_0$  (a geometrical shape factor of 1.15 is a typical value for an I-profile and 1.5 for a solid beam).

A different picture arises when we do not look at the rotation capacity  $R$ , but rather at the curvature capacity  $R_k$ . Figures 5c and 5d, show the same results as in figures 5a and 5b, but now in terms of the curvature capacity. A distinct influence of the strain-hardening potential is present, especially for the more optimized cross-sectional shapes as common for aluminium design and as indicated with a low value for the generalized shape factor  $a_0$ . Because the curvature is less localized for aluminium alloys at elevated temperatures which have a greater strain hardening potential, a lower maximum curvature is required for a plastic mechanism to form.

#### 4 Example

To demonstrate the effect of the phenomena described in this article, we may take a look at figure 5a and lookup the  $|M1/M2|$  ratio belonging to a stable rotation capacity of  $R_0 = 3$  as specified by (EN 1999-1-1, 2007). The maximum  $|M1/M2|$  is equal to approximately 4. Aluminium alloy 6060-T66 has a minimum quoted value of  $n = 16$  at room temperature, and this is reduced to  $n_\theta = 5$  at a temperature of 350°C. If we look up the curvature capacity requirements for  $|M1/M2| = 4$  in figure 5c, the curvature requirement is reduced from  $R_k \approx 13$  to  $R_k \approx 5$  as the temperature is increased from room temperature to 350°C. Through equation (17) and (20), it can then be calculated that the limit for the  $b/t$  ratio  $\beta$  is increased by 53% due to the diminished ductility demand, and a further 42% due to the increased  $k$ -part of equation (17). These numbers are obtained for the analytical form of equation (14). A similar increase is observed for the numerically solved, empirical form. Then the  $b/t$  limit for a class 1 internal plate of AA6060-T66 is equal to 12.2, which is increased to 17.5 at 350°C due to the decreased ductility demand. The increased stiffness over strength ratio at elevated temperatures further increases the limit for class 1 of this specific alloy at 350°C to 24.9, which is higher than the limit for class 3 at room temperature.

## 5 Conclusions

An explorative study has been performed to investigate the potential for a cross-sectional classification system for beams in fire that better reflects the actual behaviour of such beams in practice as compared to the current design rules as given in the Eurocode for fire design (EN 1999-1-2, 2007). It has been found that such potential exists and a simple equation is given to increase the geometric limits of class 2 and 3 sections, such that beams may be considered to be of a higher class in fire design. This is caused by the stiffness decreasing more slowly at an increase in temperature than the strength.

The rotational capacity requirements of class 1 sections have been investigated and it has been found that the curvature capacity demand is decreased at elevated temperatures due to the increase in strain-hardening potential and the decrease in curvature localization. At the same time the curvature resistance is actually increased due to the increase in stability, which is again caused by the stiffness decreasing more slowly at an increase in temperature than the strength. Cross-sections that are of class 2 or higher at room temperature may thus be able to sustain sufficient plastic deformation to allow a plastic calculation according to the rules of class 1 as defined by (EN 1999-1-1, 2007).

### *Acknowledgement*

This research was carried out under project number M81.1.108306 in the framework of the research program of the Materials innovation institute M2i ([www.m2i.nl](http://www.m2i.nl)).

## References

- Cappelli, M., A. De Martino, and F. M. Mazzolani (1987). Ultimate bending moment evaluation for aluminium alloy members. In R. Narayanan (Ed.), *Proceedings of the international conference on steel and aluminium structures, Cardiff, UK, 8-10 July 1987.*, Volume Aluminium structures, Essex, United Kingdom, pp. 126–134. Elsevier Applied Science publishers.
- De Matteis, G., R. Landolfo, and M. Manganiello (2003). A new classification criterion for aluminium cross-sections. In G. J. Hancock, M. A. Bradford, T. J. Wilkinson, B. Uy, and K. J. R. Rasmussen (Eds.), *Proceedings of the international conference on advances in structures (ASSCA '03), Sydney, Australia, 22-25 June 2003*, Volume 1, Lisse, the Netherlands, pp. 433–441. A.A. Balkema.

- EN 1999-1-1 (2007, May). *Eurocode 9: Design of aluminium structures - Part 1-1: General structural rules*. Brussels, Belgium: European Committee for Standardization.
- EN 1999-1-2 (2007, February). *Eurocode 9: Design of aluminium structures - Part 1-2: Structural fire design*. Brussels, Belgium: European Committee for Standardization.
- Faella, C., F. M. Mazzolani, V. Piluso, and G. Rizzano (2000, March). Local buckling of aluminium members: Testing and classification. *Journal of Structural Engineering* 126(3), 353–360.
- Lundberg, S. (2003, August). Background document: Classification of cross-section classes in fire design. Technical Report CEN/TC 250/SC 9/PT Fire/N 26, European Committee for Standardization (CEN), Brussels, Belgium.
- Maljaars, J. (2008, March). *Local buckling of slender aluminium sections exposed to fire*. Ph. D. thesis, Eindhoven University of Technology.
- Maljaars, J., F. Soetens, and H. H. Snijder (2010, January). Local buckling of fire-exposed aluminum members—A new design model. *Journal of Structural Engineering* 136(1), 66–75.
- Mazzolani, F. M., C. Faella, V. Piluso, and G. Rizzano (1996). Experimental analysis of aluminium alloy SHS-member subjected to local buckling under uniform compression. In E. de M. Batista and R. C. Batista (Eds.), *Stability problems in designing, construction and rehabilitation of metal structures: Proceedings of the 5th international colloquium on structural stability, SSRC Brazilian session, Rio de Janeiro, August 5-7 1996*, Rio de Janeiro, Brazil, pp. 475–488. Universidade Federal do Rio de Janeiro. Coordenação dos Programas de Pós-Graduação de Engenharia: COPPE/UFRJ.
- Mazzolani, F. M. and V. Piluso (1995, May). Prediction of the rotation capacity of aluminium alloy beams. In *Proceedings of: International Conference on Steel and Aluminium Structures (ICSAS)*, Istanbul, Turkey.
- Moen, L. A. (1999, January). *Rotation capacity of aluminium alloy beams*. Ph. D. thesis, Norwegian University of Science and Technology, Department of Structural Engineering, N-7034, Trondheim, Norway.
- Ramberg, W. and W. R. Osgood (1943, July). Description of stress-strain curves by three parameters. Technical Report NO. 902, National Advisory Committee for Aeronautics, Washington D.C., United States.

## List of symbols

$\varepsilon$	Strain
$\varepsilon_{0.2}$	Strain at the 0.2% proof stress
$\varepsilon_{cr}$	Critical elastic strain
$\varepsilon_{lb}$	Strain at local buckling (inelastic)
$\kappa$	Curvature
$\kappa_{0.2}$	Curvature at conventional elastic moment
$\kappa_{lb}$	Curvature at local buckling (inelastic)
$\sigma$	Stress
$\nu$	Poisson's ratio
$a_0$	Geometrical shape factor ( $W_{pl}/W_{el}$ )
$b$	Plate width
$f_{0.2}$	0.2% proof stress
$f_d$	Design value of 0.2% proof stress
$M_{0.2}$	Conventional elastic moment
$M_1$	Elastic moment at the place of the first yielding plastic hinge(s)
$M_2$	Elastic moment at the place of the yielding of a second (set of) plastic hinge(s)
$M_u$	Ultimate moment
$M_{rd}$	Design value for moment resistance
$n$	Exponent in Ramberg-Osgood equation, expressing strain-hardening ability
$R$	Rotation capacity
$R_0$	Stable rotation capacity
$R_x$	Curvature capacity
$t$	Plate thickness
$W_{el}$	Elastic section modulus
$W_{pl}$	Plastic section modulus

